JACS
JOURNAL OF THE AMERICAN CHEMICAL SOCIETY
Article
pubs.acs.org/JACS

Reversible Photoinduced Reductive Elimination of H_2 from the Nitrogenase Dihydride State, the $E_4(4H)$ Janus Intermediate

Dmitriy Lukoyanov,[†] Nimesh Khadka,[§] Zhi-Yong Yang,[§] Dennis R. Dean,[#] Lance C. Seefeldt,*[,§] and Brian M. Hoffman*[,†]

[†]Department of Chemistry, Northwestern University, Evanston, Illinois 60208, United States
[§]Department of Chemistry and Biochemistry, Utah State University, Logan, Utah 84322, United States
[#]Department of Biochemistry, Virginia Tech, Blacksburg, Virginia 24061, United States

Supporting Information

ABSTRACT: We recently demonstrated that N_2 reduction by nitrogenase involves the obligatory release of one H_2 per N_2 reduced. These studies focus on the $E_4(4H)$ "Janus intermediate", which has accumulated four reducing equivalents as two [Fe-H-Fe] bridging hydrides. $E_4(4H)$ is poised to bind and reduce N_2 through reductive elimination (*re*) of the two hydrides as H_2, coupled to the binding/reduction of N_2. To obtain atomic-level details of the *re* activation process, we carried out *in situ* 450 nm photolysis of $E_4(4H)$ in an EPR cavity at temperatures below 20 K. ENDOR and EPR measurements show that photolysis generates a new FeMo-co state, denoted $E_4(2H)$*, through the photoinduced *re* of the two bridging hydrides of $E_4(4H)$ as H_2. During cryoannealing at temperatures above 175 K, $E_4(2H)$* reverts to $E_4(4H)$ through the oxidative addition (*oa*) of the H_2. The photolysis quantum yield is temperature invariant at liquid helium temperatures and shows a rather large kinetic isotope effect, KIE = 10. These observations imply that photoinduced release of H_2 involves a barrier to the combination of the two nascent H atoms, in contrast to a barrierless process for monometallic inorganic complexes, and further suggest that H_2 formation involves nuclear tunneling through that barrier. The *oa* recombination of $E_4(2H)$* with the liberated H_2 offers compelling evidence for the Janus intermediate as the point at which H_2 is necessarily lost during N_2 reduction; this mechanistically coupled loss must be gated by N_2 addition that drives the *re*/*oa* equilibrium toward reductive elimination of H_2 with N_2 binding/reduction.

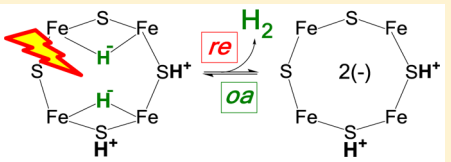

INTRODUCTION

Biological nitrogen fixation—the reduction of N_2 to two NH_3 molecules—is primarily catalyzed by the Mo-dependent nitrogenase. This enzyme comprises two component proteins, denoted the Fe protein and the MoFe protein. The former delivers electrons one at a time to the MoFe protein, where they are utilized at the active-site iron−molybdenum cofactor ([7Fe-9S-Mo-C-*R*-homocitrate]; FeMo-co, Figure 1) to reduce substrate.[1,2] Kinetic studies of N_2 reduction by nitrogenase, carried out in the 1970s and 1980s by many groups, especially by Lowe and Thorneley and their co-workers, culminated in the Lowe−Thorneley (LT) kinetic model for nitrogenase function.[1,3,4] It describes the kinetics of transformations among catalytic intermediates, denoted E_n, where n is the number of electron/proton deliveries to the catalytic FeMo-co, with electron transfer from the partner Fe protein in each of these steps being driven by the binding and hydrolysis of two MgATPs within the Fe protein.[5] A central defining feature of this scheme is a mysterious and puzzling, obligatory (mechanistic) requirement for the formation of one H_2 for each N_2 reduced. This, in turn, leads to a limiting eight-electron enzymatic stoichiometry for enzyme-catalyzed nitrogen fixation, eq 1, a conclusion in agreement with stoichiometric experiments by Simpson and Burris.[6] However, the obligatory requirement for H_2 formation has not been universally accepted.[7] Most tellingly, in their magisterial review, Burgess and Lowe themselves questioned this requirement:[1] "Thus, the data that support the obligatory evolution of one H_2 for every N_2 reduced are much less compelling than the data that require us to believe that some H_2 will always be evolved during N_2 reduction."

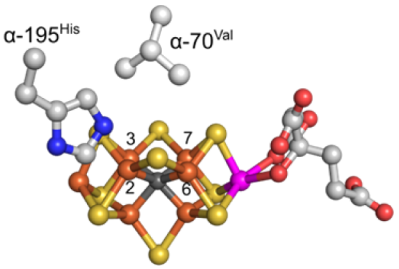

Figure 1. Crystal structure of FeMo-co. Fe is shown in rust, Mo in magenta, S in yellow, carbide in dark gray, C in gray, N in blue, and O in red. The Fe-atoms of the catalytic 4Fe-4S face are labeled as 2, 3, 6, and 7. Two amino acids, α-70^{Val} and α-195^{His}, around the FeMo-co are also shown; either just the former or both are modified in the enzyme used in this study (see text). The image was created using coordinates for PDB 2AFI.

Received: November 6, 2015
Published: January 20, 2016

DOI: 10.1021/jacs.5b11650
J. Am. Chem. Soc. 2016, 138, 1320−1327

$$N_2 + 8e^- + 16ATP + 8H^+ \rightarrow 2NH_3 + H_2 + 16ADP + 16P_i \quad (1)$$

We recently proposed[8,9] that obligatory H_2 formation was required to explain the multitude of mechanistic observations by numerous investigators that had accumulated over decades.[1] This proposal focuses on the $E_4(4H)$ "Janus intermediate" (see Figure 2 for notation), which has accumulated four of the eight

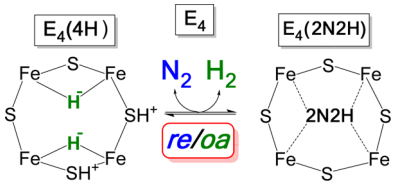

Figure 2. Schematic of *re/oa* equilibrium. The cartoon represents the Fe 2, 3, 6, and 7 faces of FeMo-co, and "2N2H" implies a species at the diazene reduction level of unknown structure and coordination geometry. In the indicated equilibrium, the binding and activation of N_2 are mechanistically coupled to the *re* of H_2, as described in the text. In the E_n notation, n = number of e^-/H^+ added to FeMo-co; parentheses denotes the stoichiometry of H/N bound to FeMo-co.

required reducing equivalents, storing them as two [Fe-H-Fe] bridging hydrides.[10−12] $E_4(4H)$ sits at a transition in the N_2 reduction pathway, poised to "fall back" to E_0 by release of two H_2, but equally poised to bind and reduce N_2 through the accumulation of four more equivalents, hence the appellation.[9] The bridging mode of hydride binding plays a key mechanistic role. Bridging hydrides are less susceptible to protonation than terminal hydrides, and so they diminish the tendency of FeMo-co to "fall back" by losing reducing equivalents through the formation of H_2. However, the bridging mode also lowers hydride reactivity relative to that of terminal hydrides.[13,14] How this "deactivated" intermediate becomes activated through the release of H_2 coupled to N_2 binding forms part of the "mystery" of dinitrogen fixation by nitrogenase.

We proposed that the $E_4(4H)$ state becomes activated for the binding of N_2 and its hydrogenation to a N_2H_2-level moiety through the reductive elimination (*re*) of the two hydrides as H_2, the forward direction of the equilibrium in Figure 2.[8,9] This proposal was initially supported[8,9] by showing that the behavior of nitrogenase during the reverse of this equilibrium, the oxidative addition (*oa*) of H_2 with loss of N_2, explains the key constraints on nitrogenase mechanism that had been revealed over the years.[1] In particular it explains the previously baffling observation that D_2 can only react with nitrogenase during turnover with N_2 present, and then is stoichiometrically reduced to two HD.[1] Promptly thereafter we confirmed the mechanistic prediction that during turnover under N_2/D_2, the reverse of the equilibrium of Figure 2, the *oa* of D_2 by the $E_4(2N2H)$ intermediate with the loss of N_2, must generate the $E_4(2D2H)$ isotopologue with D_2 having been converted selectively into two bridging deuterides, a state which could form in no other way.[15] This observation established the *re/oa* equilibrium is thermodynamically reversible. More recently, we demonstrated that the (*re/oa*) activation equilibrium of Figure 2 is not only thermodynamically, but also kinetically reversible. The overall result of these several findings is to establish the mechanistic requirement for the formation of one H_2 per N_2. This in turn implies the limiting stoichiometry of eight electrons/protons for the reduction of N_2 to two NH_3 (eq 1).[16]

But these efforts, while establishing the *re/oa* mechanism for nitrogenase activation, do not provide atomic-level details of the *re* activation process. For example, in rough analogy to nucleophilic substitution in organic chemistry, we can imagine a spectrum of reaction pathways for *re/oa*, as illustrated in Figure 3: Is

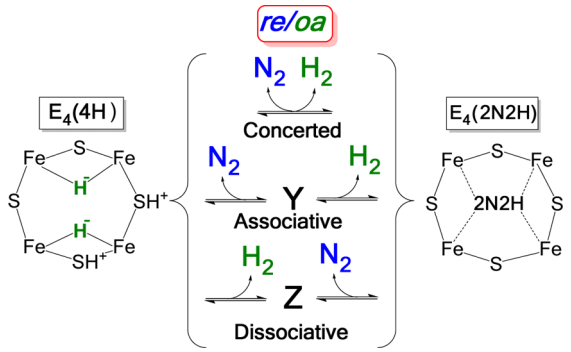

Figure 3. Schematic of alternative limiting mechanisms for *re/oa* equilibrium.

the conversion concerted? Associative? Dissociative? If a discrete intermediate (e.g., **Y**, or **Z**) exists, what are its properties? To obtain atomic-level details of the *re* activation process requires deeper understanding of the inorganic chemistry of the bridging hydrides of $E_4(4H)$: What are their properties, and what properties do they confer on this enzyme state? We here present the initial results of a photochemical approach inspired by the properties of inorganic dihydride complexes.

The photolysis of transition metal dihydride complexes with mutually *cis* hydride ligands commonly results in the release of H_2.[17−26] As noted by Perutz,[17] "The photochemical reaction causes a reduction in oxidation state of two and is a typical example of reductive elimination. The reverse reaction will usually proceed thermally and is the prototype example of an oxidative addition reaction." Regardless of the precise nature of the thermal *re/oa* equilibrium process in nitrogenase (Figure 2), photoinduced *re* would cleanly give an activated version of the doubly reduced $E_2(2H)$ intermediate, which we denote $E_4(2H)^*$, that would be analogous to the intermediate that would form upon thermal dissociative *re* loss of H_2 prior to N_2 binding (**Z**, Figure 3). Our cartoon depictions of $E_4(4H)$ frequently have shown the two [Fe−H−Fe] hydrides with a common vertex (see Chart 1) in order to emphasize the analogy between *re* of H_2 by

Chart 1

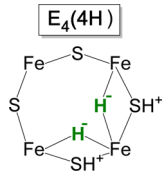

mononuclear metal dihydrides, and the activation of FeMo-co through *re* of H_2. However, we do not yet know their exact disposition, and know of no precedent for *re*, either thermal or photochemical, for the "parallel" hydrides drawn in the cartoon (Figure 2), a geometry that is suggested by preliminary DFT computations.[27] On the other hand, no inorganic multimetallic dihydride of which we are aware exhibits a 4Fe "face", as does

DOI: 10.1021/jacs.5b11650
J. Am. Chem. Soc. 2016, 138, 1320−1327

FeMo-co, and therefore none could have the adjacent, parallel hydrides drawn in the cartoon. Thus, photolysis of the Janus $E_4(4H)$ intermediate embeds FeMo-co even more deeply within the body of organometallic chemistry, yet breaks new ground.

MATERIALS AND METHODS

Materials and Protein Purifications. All the reagents were obtained from SigmaAldrich (St. Louis, MO) or Fisher Scientific (Fair Lawn, NJ) and were used without further purification. Argon, N_2, and acetylene gases were purchased from Air Liquide America Specialty Gases LLC (Plumsteadville, PA).

Remodeling the active site of MoFe protein by the α-$70^{Val\rightarrow Ile}$ mutation permits the freeze trapping of MoFe with high populations of $E_4(4H)$.[10] Experiments were carried out both with the singly substituted, α-70^{Ile} MoFe protein and with the doubly substituted α-$70^{Val\rightarrow Ile}$/α-$195^{His\rightarrow Gln}$ MoFe proteins. As shown in Table S1, this protein functions similarly to the single mutant. The two proteins were obtained from the corresponding *Azotobacter vinelandii* strains. They were grown, and the corresponding nitrogenase MoFe proteins were expressed and purified as described elsewhere.[28] The handling of all buffers and proteins were done anaerobically under Ar atmosphere or under Schlenk vacuum line unless stated otherwise.

EPR and ENDOR Samples. The $E_4(4H)$ intermediate and its deuterated analogue, $E_4(4D)$, are prepared by turnover of the MoFe protein in H_2O and D_2O buffers, respectively. Depending on the buffer used, all exchangeable sites are thereby populated with H or D, not only the hydride bridges. Thus, measured kinetic isotope effects associated with *re* and *oa* steps of the equilibrium of Figure 2[29,30] are a composite of primary isotope effects associated with hydride *re* or H_2 *oa* plus any, smaller, solvent isotope effects.

EPR samples were prepared in a dioxygen free buffer containing a MgATP regeneration system with final concentrations of 13 mM ATP, 15 mM $MgCl_2$, 20 mM phosphocreatine, 2.0 mg/mL bovine serum albumin, and 0.3 mg/mL phosphocreatine kinase in a 200 mM MOPS buffer at pH 7.3 (H_2O buffer) or pD 7.3 (D_2O buffer; pH meter reading of 6.9)[31] with 50 mM dithionite. MoFe protein was added at ~50 μM final concentration and the reaction was initiated by addition of Fe protein at ~36 μM concentration. The reaction was allowed to run at room temperature under Ar atmosphere for 20−25 s before freeze-quenching the samples. The samples for ENDOR experiments were prepared similarly, but typically with 3-fold higher concentrations.

EPR and ENDOR Measurements. X-band EPR spectra were recorded on a Bruker ESP 300 spectrometer equipped with an Oxford Instruments ESR 900 continuous He flow cryostat.

To allow illumination, a Bruker ER4104R cavity was employed. This cavity allows front-face optical access through a waveguide beyond cutoff (microwave non-transmitting) on the cavity front face, with a 4 × 10 mm optical transmission path. *In situ* photolysis of a sample held within the cryostat at the chosen temperature initially employed a 15 mW blue LED inserted into this illumination port. Subsequently it employed a Thorlabs Inc. (Newton, NJ) PL450B, 450 nm, 80 mW Osram Laser Diode mounted on the port through use of the corresponding diode mount with focusing lenses. Thermal relaxation was monitored by the step-annealing procedure in which the sample was quickly warmed to a desired temperature, held there for a fixed time, then promptly returned to 77 K, and then examined by EPR at a still lower temperature.

Q-band CW EPR and ^{1,2}H ENDOR spectra were collected on a spectrometer with a helium immersion Dewar as previously reported.[32] The stochastic field-modulation detected ENDOR technique, first reported by Brueggeman and Niklas,[33] was also utilized. In the stochastic ENDOR sequence, RF is randomly hopped over the frequency range of the spectrum, with subtraction of a background signal (RF off) at each frequency. All measurements were done at 2 K. As desired, Q-band samples were photolyzed by placing them in liquid nitrogen in an X-band finger Dewar and illuminating them with a 1000 mW blue LED. The samples were then transferred to a liquid helium cryostat for EPR/ENDOR study.

RESULTS AND DISCUSSION

Figures 4 and S1 present X-band and Figure S2 presents Q-band EPR spectra of the S = 1/2 $E_4(4H)$ intermediate

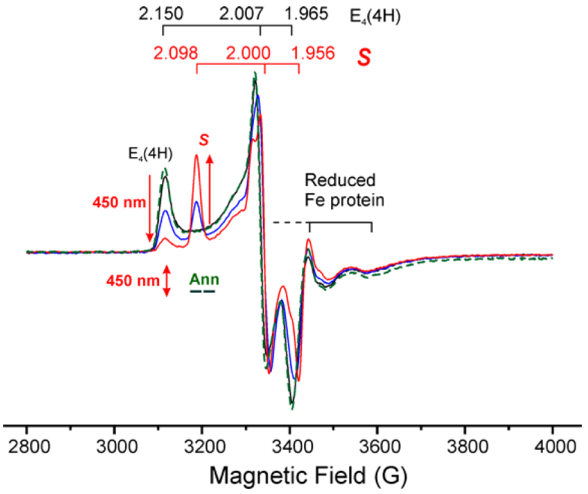

Figure 4. X-band EPR spectra of MoFe protein (α-70^{Ile}) freeze-trapped during Ar turnover in H_2O before (black) and during irradiation with 450 nm diode laser at 12 K (blue, 2.5 min, and red, 20 min traces). Red arrows highlight the conversion of $E_4(4H)$ to the photoinduced ***S*** state. Dashed green spectrum shows that annealing (Ann) the illuminated sample at 217 K for 2 min causes complete reversion of ***S*** to $E_4(4H)$. EPR conditions: T = 12 K; microwave frequency, 9.36 GHz; microwave power, 10 mW; modulation amplitude, 13 G; time constant, 160 ms; field sweep speed, 20 G/s.

freeze-trapped during turnover of MoFe protein that was remodeled with the α-$70^{Val\rightarrow Ile}$ substitution; similar results are seen for MoFe with the double substitution, α-$70^{Val\rightarrow Ile}$/α-$195^{His\rightarrow Gln}$ (Figure 1). Both single and double substitutions prevent access of substrates other than protons, without perturbing FeMo-co function (Table S1), and enhance the accumulation of $E_4(4H)$.[10−12]

Figure 4 includes spectra collected during *in situ* photolysis with 450 nm light with the sample held at 12 K; equivalent spectra are obtained by photolysis at 77 K (e.g., Figure S2). Although it has not yet proven possible to create optically transparent freeze-quenched samples of this intermediate, the figures show that irradiation nonetheless causes the progressive loss of the $E_4(4H)$ signal, $\mathbf{g}$ = [2.15, 2.007, 1.965], and accompanying appearance of a new signal, ***S***, with $\mathbf{g}$ = [2.098, 2.0, 1.956]. EPR spectra collected over temperatures between 12 and 50 K (Figure S1) show the $E_4(4H)$ signal disappears by ~40−50 K because of rapid spin relaxation, whereas for ***S***, the EPR signal is clearly visible at 50 K, demonstrating differences between excited spin-state manifolds of ***S*** and $E_4(4H)$.

Careful examination of the timecourse of photolysis shows no new signals that are generated, other than ***S***. In particular, Figures 4, S1, and S2 show *no* other photoinduced change in the spectrum in the vicinity of $g \approx 2$; likewise, there is *no* change at lower fields (not shown), where the signal from residual resting state (E_0) appears and where signals would appear from the state which has accumulated two [e^-/H^+] ($E_2(2H)$).[34] The photolysis product, ***S***, completely relaxes back to $E_4(4H)$ when annealed for 2 min at 217 K, with *no* other change in the EPR spectrum, either in the $g \approx 2$ region (Figure 4) or in the high-g (low-field) region (not shown).

DOI: 10.1021/jacs.5b11650
J. Am. Chem. Soc. 2016, 138, 1320−1327

Thus, photolysis/annealing cause the reversible conversion, $E_4(4H) \Leftrightarrow S$.

^{1,2}H ENDOR spectroscopy was used to determine the fate of the [Fe−H−Fe] bridging hydrides during the photolytic $E_4(4H) \Rightarrow S$ conversion. Figure 5 shows 2 K Q-band stochastic

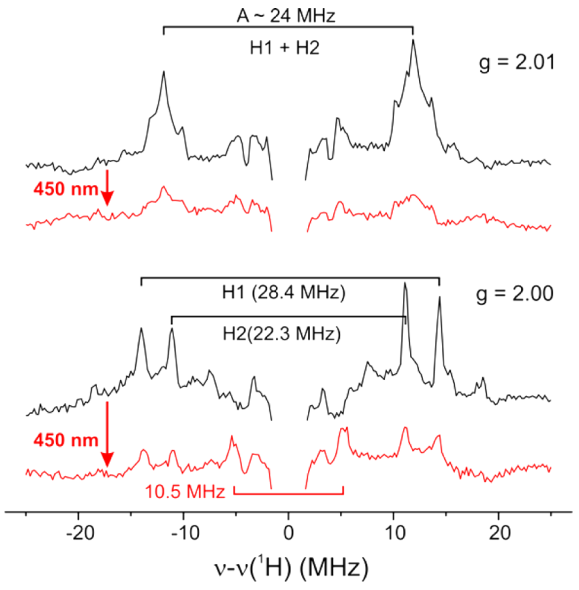

Figure 5. Q-band stochastic ^{1}H CW ENDOR spectra showing loss of signals from hydrides, H1 and H2, through photolysis. (Black) Before and (red) after 450 nm photolysis of MoFe protein (α-70^{Ile}/α-195^{Gln}) trapped during Ar turnover in H_2O buffer. ENDOR conditions: microwave frequency, ~34.99 GHz; modulation amplitude, 6.3 G; RF duration, 3 ms; RF cycle, 200 Hz; bandwidth of RF broadened to 100 kHz; 2000 scans; temperature, 2 K.

CW ^{1}H ENDOR spectra collected at two different g-values from $E_4(4H)$ before and after photolysis; Figure S2 presents corresponding "conventional" CW spectra. In both figures, the spectra represent components of the 2D field-frequency pattern of spectra collected across the EPR envelope, which has been thoroughly analyzed in terms of two hydrides with anisotropic hyperfine tensor components that are virtually identical, but with tensors that are differently oriented with respect to **g**.[10] In the g = 2.01 spectrum of $E_4(4H)$ in Figure 5, the strongly coupled ^{1}H signals from the two hydrides ($A \lesssim 40$ MHz) are completely overlapped; at g = 2.00, the signals again overlap, but distinct peaks also are seen from the individual hydrides, most noticeably the two doublets with couplings of $A \approx 22$ and 28 MHz.[10,27]

For the sample that gave the ENDOR spectra in Figure 5, the photolysis had reduced the intensity of the $E_4(4H)$ EPR signal by ~3-fold, with the corresponding appearance of EPR intensity from ***S***. Figure 5 shows that the photolysis decreases the intensity of the ^{1}H ENDOR signals from the strongly coupled hydrides by a comparable amount, *without* the appearance of new strongly coupled signals that can be associated with a metal-hydride "isomer". At g = 2.01, *no* new signal appears; at g = 2.0, a signal appears with the relatively small coupling, $A \approx 10$ MHz, which likely is associated with one of the protonated sulfides that must be present in ***S***. CW ENDOR spectra taken on a sample with an even greater extent of photolysis show essentially complete loss of the ENDOR signals at a field where the two hydrides show distinct features (Figure S2). Correspondingly, ^{2}H ENDOR measurements of ***S*** created by photolysis of $E_4(4D)$ prepared in D_2O buffer show the loss of the [Fe-D-Fe] signals associated with $E_4(4D)$, again with no new strongly coupled signal appearing (not shown).

The absence of new strongly coupled signals in the ^{1,2}H ENDOR responses further rules out the possibility that ***S*** is an H_2 complex of FeMo-co, either with strongly hindered or free rotation of H_2, rather than having released H_2. A bound H_2 complex with strongly hindered rotation would show new strongly coupled ^{1}H ENDOR signals, contrary to observation.[35] Quantum statistical arguments show that freely rotating H_2, which can occur even at 2 K, would not show ^{1}H ENDOR signals, but would show new strongly coupled ^{2}H ENDOR signals for the corresponding D_2O sample.[36] The absence of such new signals for ***S*** means that it does not contain a freely rotating bound D_2.

We thus infer that the state ***S*** generated by photolysis of $E_4(4H)$ has indeed lost the metal-bound hydrides through the release of one or two H_2.

Mechanism of Photoconversion. Three mechanisms must be considered for the $E_4(4H) \Rightarrow S$ photoconversion through loss of both hydrides and release of H_2 (Figure 6),

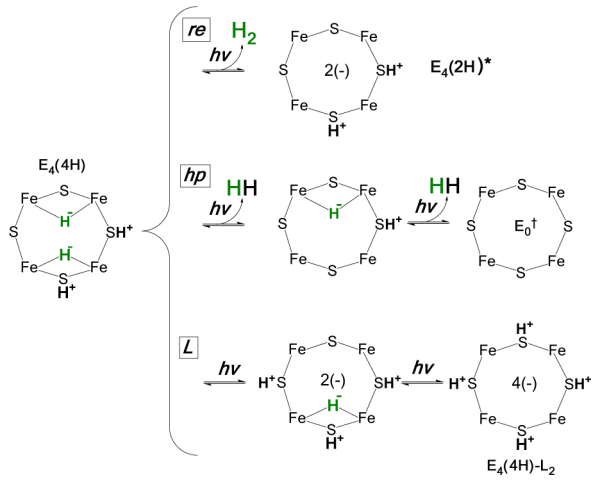

Figure 6. Alternative mechanisms for the $E_4(4H) \Rightarrow S$ photoconversion through loss of both hydrides, release of H_2, and thermal reverse.

which we denote *re*, *hp*, and *L*. The first would be precisely the photoinduced reductive-elimination of one H_2, as discussed above, yielding a nonthermal form of the doubly reduced state of the cluster, which we denote $E_4(2H)$*. The second postulates two steps of photoinduced hydride protonolysis (*hp*), each with loss of H_2, in which case ***S*** must be a low-spin (S = 1/2) "spin-isomer" of the E_0, S = 3/2 resting state, which we can denote $E_0^{\dagger}$. Thermal *hp* processes are responsible for H_2 formation by nitrogenase,[1,8,9] as well as by hydrogenases.[37,38] The third mechanism differs from the other two in that it does not involve generation of H_2. Instead it would involve two steps of photoinduced *re* of a hydride, with transfer of the proton "released" to a bridging sulfide. We denote this the "*L* mechanism" because it is inspired by the photoinduced conversion of the Ni−C state of the Ni−Fe hydrogenases.[37,38] Ni−C exhibits a [Ni(III)-H-Fe(II)] bridging hydride and a cysteinyl thiolate bound to Ni. Photolysis generates a state, denoted Ni-L, which contains [Ni(I), Fe(II)] metal ions, and with the proton formed by photoinduced reductive elimination of the hydride having been transferred to the bound sulfur.

DOI: 10.1021/jacs.5b11650
J. Am. Chem. Soc. 2016, 138, 1320−1327

Any one of these three imagined processes would yield a final photoproduct without metal hydrides.

The observation that ***S*** thermally relaxes to $E_4(4H)$ immediately rules out the *hp* mechanism for photoinduced $E_4(4H) \Rightarrow \boldsymbol{S}$ conversion. This conversion would involve the loss of four reducing equivalents as two H_2 molecules, and its reverse must involve two steps of reduction of FeMo-co by H_2: $E_0^{\dagger} + H_2 \Rightarrow E_2(2H)$; $E_2(2H) + H_2 \Rightarrow E_4(4H)$. However, it is one of the foundational facts about nitrogenase mechanism that H_2 cannot react with any thermally generated state of FeMo-co except the N_2-bound state produced by *re* of H_2; as we have explained, the reactions are uphill by ~30 kcal/mol.[8] Even if the $E_0^{\dagger}$ photogenerated spin isomer were sufficiently activated as to react with H_2, the first step of reduction would necessarily produce the thermally equilibrated $E_2(2H)$, which could not react with H_2: hence $E_4(4H)$ could not be regenerated from ***S*** during cryoannealing.

The complete absence during photolysis of a second new EPR signal in addition to ***S*** (see above) in fact not only independently rules out *hp*, but also rules out *L*. Both mechanisms involve sequential steps of photon absorption. Under the constant low-level illumination of this experiment this necessarily implies the buildup then loss of the EPR signal from the intermediate stage that has absorbed one photon. *Thus, we conclude that photolysis indeed generates a FeMo-co state,* $\boldsymbol{S} = E_4(2H)^*$*, through the photoinduced reductive elimination of the two bridging hydrides of* $E_4(4H)$ *with accompanying production of one* H_2*, and that the relaxation of* $E_4(2H)^*$ *to* $E_4(4H)$ *during cryoannealing corresponds to the oxidative addition of* H_2 *to the photogenerated state,* $E_4(2H)^*$.

Kinetics of H_2/D_2 *oa*. To characterize the isotope dependence of the thermal *oa* process, $E_4(2H)^* + H_2 \Rightarrow E_4(4H)$ versus $E_4(2D)^* + D_2 \Rightarrow E_4(4D)$,[29,30,39] we measured the kinetics of the 193 K relaxation of $E_4(2H)^*$ and $E_4(2D)^*$ in samples prepared, respectively, in H_2O and D_2O buffers. In these experiments the sample was annealed at 193 K for multiple time intervals, with cooling to 12 K for collection of EPR spectra between intervals. For both H_2O and D_2O buffers the relaxation is well-modeled as a one-step process (Figure 7). This is consistent with, but not proof of, the absence of an intermediate state(s), for example an H_2 complex.[40]

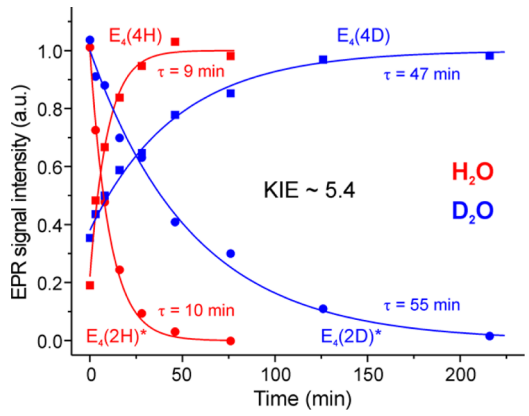

Figure 7. Decay during 193 K annealing of $E_4(2H)^*$ photoinduced in MoFe (α-70^{Ile}) freeze-trapped during turnover in H_2O (red) and D_2O (blue), along with the parallel recoveries of $E_4(4H)$. Data points obtained as intensities of g_1 feature of the corresponding $S = 1/2$ EPR signals, normalized to the maximum signal; they were fit with an exponential function, with time constants shown in the figure. EPR conditions: as in Figure 4.

With ***S*** in H_2O buffer, the exponential decay time-constant is, τ = 10 min; decay is slowed in D_2O buffer, to the decay time, τ = 55 min. The $E_4(4H)$ state recovers in synchrony with the loss of ***S***, as the recovery also is exponential, and exhibits the same time-constants, τ = 9 min for H_2O sample and τ = 47 min for D_2O. This kinetic isotope effect during *oa*, KIE ≈ 5.4, is larger than typical for closed-shell monometallic complexes.[41,42] Combined with a strong temperature dependence in the time constant (not shown), this KIE implies that *oa* of H_2 involves traversal of an energy barrier associated with H_2 binding and/or bond cleavage. The exponential decay of ***S*** and appearance of $E_4(4H)$ suggest that in the frozen solution the H_2 formed by photoinduced *re* is trapped adjacent to FeMo-co and undergoes *oa* "intramolecularly", presumably in some part because the incorporation of isoleucine over the active face of FeMo-co prevents H_2 diffusion away. Indeed, although we presume that the relatively weakly coupled, but clearly resolved ^{1}H ENDOR signal seen for ***S*** is associated with a sulfur-bound proton, we cannot rule out the possibility that it comes from the H_2 trapped nearby.

KIE of Photoinduced *re*. We know of only two studies of the KIE for photoinduced *re* of H_2/D_2, and these found small[43] or negligible isotope effects.[21] For completeness, we nonetheless used *in situ* photolysis to compare the time-dependent loss of the $E_4(4H)$ and corresponding $E_4(4D)$ signals as a function of temperature (Figure 8). In a clear solution of low optical

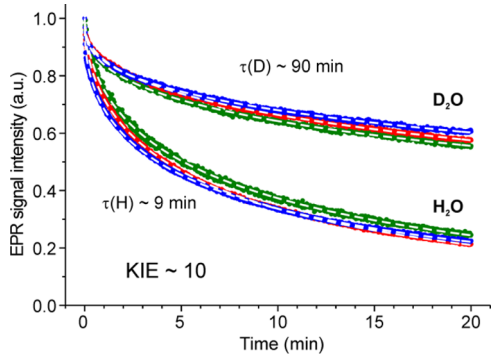

Figure 8. Time course of *in situ* 450 nm photoinduced conversion of $E_4(4H)$ intermediate trapped during MoFe protein (α-70^{Ile}) turnover in H_2O (lower) and D_2O (upper). Photolysis at 3.8 (green), 8 (red), and 12 K (blue). Signal measured directly as intensity of the g_1 feature of the $E_4(4H)$ $S = 1/2$ EPR signal, normalized to the maximum signal and fit with a stretched exponential decay function, $I = \exp(-[t/\tau]^n)$, with "1/e" time constant τ; $0 < n \leq 1$ equals unity for exponential decay and decreases with the spread of the distribution. Time constants for fits (*white* dashed lines) are given in figure; in all cases $n \approx 0.4$ (see SI for details). EPR conditions: microwave frequency, 9.36 GHz; microwave power, 10 mW (1 mW for measurements at 3.8 K); modulation amplitude, 13 G; time constant, 160 ms.

density, photolysis under constant illumination would cause an exponential loss of the signal with rate constant (k) proportional to the light intensity (I_0) and quantum yield (ϕ), for *re*, $k(\phi) = \tau^{-1}(\phi) \propto I_0\phi$, where $\tau(\phi)$ is the corresponding time-constant for decay. However, it proved impossible to prepare clear frozen samples with high population of $E_4(4H)$, only frozen "snows". The decay of the signal during photolysis of a "snow" is *necessarily* nonexponential because light scattering diminishes the photon flux across the sample (see SI); instead, as shown in Figure 8, it can be described with a stretched exponential, $\exp(-[t/\tau]^n)$,[44] with ϕ-dependent "1/e" decay

DOI: 10.1021/jacs.5b11650
J. Am. Chem. Soc. 2016, 138, 1320−1327

time, $\tau(\phi)$, whose inverse is proportional to the average decay rate constant $(\bar{k})$[44] and is thus proportional to the quantum yield for *re*: $\tau^{-1}(\phi) \propto \bar{k}(\phi) \propto \phi$ (see SI).

The decay time for photoinduced *re* of dihydrogen from $E_4(4H)$ measured in *both* H_2O and D_2O buffers is temperature invariant, within error, from 4 to 12 K (Figure 8, Table S2), a variation in the thermal energy (k_BT) by a factor of ~3. Contrary to expectation, the decay slows markedly in D_2O buffer; the KIE for *re* over this range, defined as the ratio of the "1/e" decay times for D_2O and H_2O buffers, is large, KIE ≈ 10. *These observations together imply that photoinduced re involves a barrier to the combination of the two nascent H atoms, in contrast to the barrierless process inferred for monometallic metal complexes,*[17,21] *and suggest that the photoinduced formation of* H_2 *involves nuclear tunneling through that barrier.* Whether the process involves an actual intermediate H_2 complex remains to be determined. In combination with the evidence for a barrier crossing in the *oa* of H_2 to $E_4(2H)^*$ to regenerate $E_4(4H)$, this leads us to the picture of the energy surfaces for photoinduced *re/oa* for the Janus intermediate presented in Figure 9.

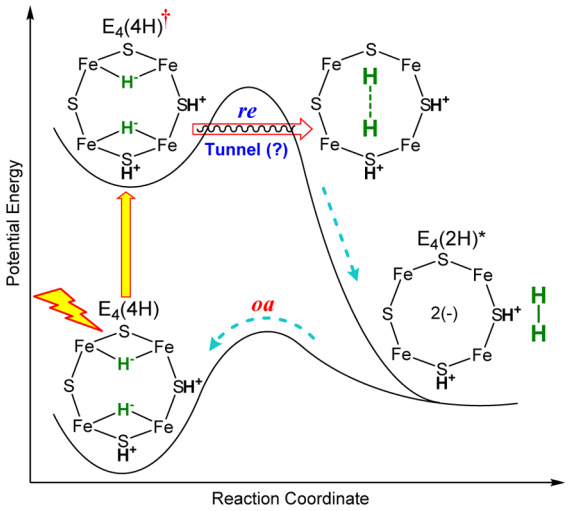

Figure 9. Idealized energy surfaces for photoinduced *re/oa* of the Janus intermediate, $E_4(4H)$. Among issues to be resolved are the possibility of tunneling on the excited-state surface, "(?)", and whether there are stable intermediates along *re* or *oa* paths.

Second Channel for Photoinduced Reaction. Intriguingly, the slowed conversion of $E_4(4D)$ to $E_4(2D)^*$ in D_2O buffer uncovered a second channel for the photoinduced loss of $E_4(4D)$, one which could not compete with the more rapid conversion to $E_4(2H)^*$ in H_2O. During photolysis of $E_4(4D)$ in D_2O buffer at ~10 K we observed a very weak photoinduced spin $S = 1/2$ EPR signal in addition to that of $E_4(2D)^*$ (not shown). This state is much less stable than $E_4(2D)^*$, and decays completely within 2 min upon raising the temperature to 77 K. Its low population and instability have precluded detailed analysis, and it has proven impossible to determine its mechanism of formation (for example, whether it is generated by the *L* mechanism).

Excited-State Molecular Orbitals. The photoinduced *re* of mutually *cis* hydrides on a single metal ion (M) has been studied computationally[45,46] and is thought to occur from a ligand-field excited state that is H-H bonding and that weakens M-(H-H) bonding and/or is actually M-(H-H) (σ^*) antibonding, as shown in Figure 10. The process is thought to

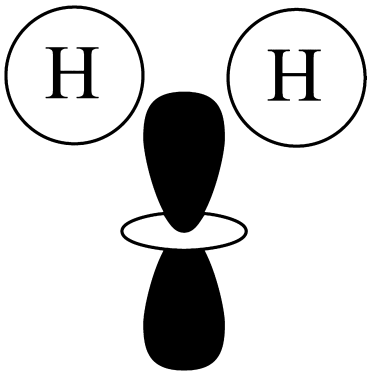

Figure 10. Cartoon showing nodal properties of an excited MO for an $M(H)_2$ complex that is bonding between the two hydrides and antibonding between each one and the metal d_{z^2} orbital.

be concerted, and to occur on a barrierless repulsive energy surface, with the H's freely coming together for release as H_2.[17,21] This view is compatible with measurements showing prompt release of H_2 after photolysis (<6 ps),[18] and with the absence of a KIE for H_2/D_2 photorelease.[21] The large KIE and tunneling-like behavior for the photo-*re* of $E_4(4H)$ in contrast imply that its excited energy surface must instead have a barrier to H_2 formation, and suggest that at the low temperature of our experiments H_2 is formed by H-atom tunneling through the barrier. This behavior in turn suggests to us that the hydrides of $E_4(4H)$ do not have a common vertex.

What type of excited state can generate the release of bridging hydrides? Regardless of whether the two bridging hydrides share a vertex (Chart 1) or are otherwise displayed, as in the "parallel" arrangement in Figures 2, 3, and 6, by analogy to the mononuclear case we would suggest that the optical excitation generates a M_2-(H-H) (σ^*) antibonding ligand-field excited state of one of the two bridging hydrides, as exemplified in Figure 11. This could couple to the equivalent state of the

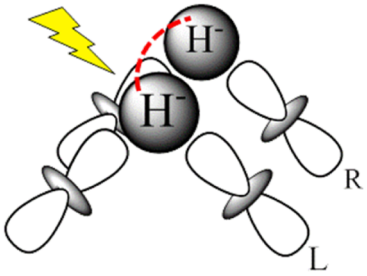

Figure 11. Cartoon showing nodal properties of the excited MOs for bridging hydrides (parallel arrangement), each antibonding between the hydride and the two d_{z^2} orbitals on the Fe ions it bridges.

other bridging hydride, delocalizing the excitation and generating a *cluster* excited state from which H_2 is liberated, or alternatively, the excited hydride state might undergo reductive elimination through an L-like mechanism, with the "liberated" proton attacking its neighbor hydride, liberating H_2. In any case, the formation of H_2 appears to involve nuclear tunneling through a barrier, as discussed above.

■ SUMMARY AND PROSPECTS

These measurements have shown that *in situ* 450 nm photolysis of the Janus intermediate, $E_4(4H)$, in an EPR cavity at temperatures below 20 K generates a new FeMo-co state, denoted $E_4(2H)^*$,

DOI: 10.1021/jacs.5b11650
J. Am. Chem. Soc. 2016, 138, 1320−1327

that has lost the hyperfine couplings characteristic of the two bridging hydrides. We have concluded that this state is neither a "hydride isomer" nor an H_2 complex, but instead $E_4(4H)$ has undergone photoinduced *re* of the two bridging hydrides of $E_4(4H)$ to generate $E_4(2H)$* with the release of H_2. During cryoannealing at temperatures above 175 K, $E_4(2H)$* reverts to $E_4(4H)$ through the oxidative addition (*oa*) of H_2. Our observations further imply that photoinduced release of H_2 involves a barrier to the combination of the two nascent H atoms, in contrast to a barrierless process for monometallic inorganic complexes, and further suggest that H_2 formation involves nuclear tunneling through that barrier. The *oa* recombination of $E_4(2H)$* with the liberated H_2 offers compelling evidence for the Janus intermediate as the point at which H_2 is necessarily lost during N_2 reduction; this mechanistically coupled loss must be gated by N_2 addition that drives the *re/oa* equilibrium toward reductive elimination of H_2 with N_2 binding/reduction.[47]

There are many issues to be addressed concerning this remarkable observation of photoinduced *re* of the bridging hydrides of $E_4(4H)$ and its thermal reverse, *oa* of H_2 by the photogenerated $S = E_4(2H)$* intermediate. Most obvious is further characterization of the energy surfaces for photoinduced *re/oa* of the Janus intermediate, $E_4(4H)$, through experiments that address the indications of tunneling during photoinduced *re* and the possibility of stable intermediates during either *re* or *oa* or both, as noted in the legend to Figure 9. In addition, we anticipate characterizing $E_4(2H)$* by ^{57}Fe and ^{95}Mo ENDOR spectroscopy.

Expanding the perspective, it is of particular interest to examine the reactivity of the photogenerated state $E_4(2H)$*. We know that $E_4(2H)$* is in some way more reactive than all thermally generated states of FeMo-co *except* the $E_4(2N2H)$ state produced by *re* of H_2 (Figure 2), as this latter is the only turnover state that can react with H_2, through the *oa* reverse of the *re/oa* equilibrium with loss of N_2. It seems unlikely that this equilibrium in fact involves the dissociative pathway of Figure 3, as $E_4(4H)$ *re* does not occur unless N_2 is present. Nevertheless, it is important to test whether $E_4(2H)$* binds and reacts with N_2, as would be the case if *re* did occur in this fashion and $E_4(2H)$* were equivalent to **Z** (Figure 3). Indeed, as there is keen interest in using nitrogenase to reduce substrates other than N_2,[48−50] it is of fundamental importance to test if $E_4(2H)$* can react with other possible substrates (CO_2, C_2H_2, C_2H_4, etc.), as occurs with the coordinatively unsaturated states produced by photo-*re* of single-metal complexes.[17,20,51]

Of course, the use of α-70^{Ile} MoFe protein precludes such experiments. Although this active-site change is central to the present report in allowing the accumulation of high populations of $E_4(4H)$, it does so at the cost of blocking access to the FeMo-co active site to all substrates *but* protons.[10] There is, however, an excellent prospect of overcoming this limitation. We find that under certain conditions of turnover with the wild-type enzyme, the $E_4(4H)$ EPR signal can be observed. Efforts are under way to maximize its population; photochemical studies of this state will be undertaken subsequently. These may help us to distinguish between the alternative concerted and associative mechanisms for *re/oa*, as shown in Figure 3.

■ ASSOCIATED CONTENT

Supporting Information

The Supporting Information is available free of charge on the ACS Publications website at DOI: 10.1021/jacs.5b11650.

Figures S1 and S2, showing EPR and ENDOR spectra; analysis of the rate constant for photolysis in a scattering medium; and Tables S1 and S2, listing specific activities of MoFe protein variants and rate parameters for photoinduced *re* of $E_4(4H)$ (PDF)

■ AUTHOR INFORMATION

Corresponding Authors

*lance.seefeldt@usu.edu

*bmh@northwestern.edu

Notes

The authors declare no competing financial interest.

■ ACKNOWLEDGMENTS

This work was funded by the NIH (GM 111097, B.M.H.), NSF (MCB 1118613, B.M.H.), and the Department of Energy, Office of Basic Energy Sciences (L.C.S. and D.R.D.). D.L. dedicates this work to Dr. Igor N. Kurkin on the occasion of his 75th birthday.

■ REFERENCES

(1) Burgess, B. K.; Lowe, D. J. *Chem. Rev.* **1996**, *96*, 2983.

(2) Seefeldt, L. C.; Hoffman, B. M.; Dean, D. R. *Annu. Rev. Biochem.* **2009**, *78*, 701.

(3) Thorneley, R. N. F.; Lowe, D. J. *Met. Ions Biol.* **1985**, *7*, 221.

(4) Wilson, P. E.; Nyborg, A. C.; Watt, G. D. *Biophys. Chem.* **2001**, *91*, 281.

(5) Duval, S.; Danyal, K.; Shaw, S.; Lytle, A. K.; Dean, D. R.; Hoffman, B. M.; Antony, E.; Seefeldt, L. C. *Proc. Natl. Acad. Sci. U. S. A.* **2013**, *110*, 16414.

(6) Simpson, F. B.; Burris, R. H. *Science* **1984**, *224*, 1095.

(7) For example, during the decades after the definitive formulation of the LT scheme (ref 3), with its obligatory loss of H_2 and resulting eight-electron/proton stoichiometry (eq 1), numerous computational studies described "mechanisms" with only six electrons/protons. Indeed, one investigator published multiple six-electron/proton mechanisms without acknowledging or addressing the contradiction to LT: e.g., Dance, I. *Chem. - Asian J.* **2007**, *2*, 936.

(8) Hoffman, B. M.; Lukoyanov, D.; Yang, Z. Y.; Dean, D. R.; Seefeldt, L. C. *Chem. Rev.* **2014**, *114*, 4041.

(9) Hoffman, B. M.; Lukoyanov, D.; Dean, D. R.; Seefeldt, L. C. *Acc. Chem. Res.* **2013**, *46*, 587.

(10) Igarashi, R. Y.; Laryukhin, M.; Dos Santos, P. C.; Lee, H. I.; Dean, D. R.; Seefeldt, L. C.; Hoffman, B. M. *J. Am. Chem. Soc.* **2005**, *127*, 6231.

(11) Lukoyanov, D.; Yang, Z.-Y.; Dean, D. R.; Seefeldt, L. C.; Hoffman, B. M. *J. Am. Chem. Soc.* **2010**, *132*, 2526.

(12) Lukoyanov, D.; Barney, B. M.; Dean, D. R.; Seefeldt, L. C.; Hoffman, B. M. *Proc. Natl. Acad. Sci. U. S. A.* **2007**, *104*, 1451.

(13) Crabtree, R. H. *The organometallic chemistry of the transition metals*, 5th ed.; Wiley: Hoboken, NJ, 2009.

(14) Peruzzini, M., Poli, R., Eds. *Recent Advances in Hydride Chemistry*; Elsevier Science B.V.: Amsterdam, The Netherlands, 2001.

(15) Yang, Z.-Y.; Khadka, N.; Lukoyanov, D.; Hoffman, B. M.; Dean, D. R.; Seefeldt, L. C. *Proc. Natl. Acad. Sci. U. S. A.* **2013**, *110*, 16327.

(16) Lukoyanov, D.; Yang, Z. Y.; Khadka, N.; Dean, D. R.; Seefeldt, L. C.; Hoffman, B. M. *J. Am. Chem. Soc.* **2015**, *137*, 3610.

(17) Perutz, R. N. *Pure Appl. Chem.* **1998**, *70*, 2211.

(18) Colombo, M.; George, M. W.; Moore, J. N.; Pattison, D. I.; Perutz, R. N.; Virrels, I. G.; Ye, T. Q. *J. Chem. Soc., Dalton Trans.* **1997**, 2857.

DOI: 10.1021/jacs.5b11650
J. Am. Chem. Soc. 2016, 138, 1320−1327

(19) Whittlesey, M. K.; Mawby, R. J.; Osman, R.; Perutz, R. N.; Field, L. D.; Wilkinson, M. P.; George, M. W. *J. Am. Chem. Soc.* **1993**, *115*, 8627.
(20) Ballmann, J.; Munha, R. F.; Fryzuk, M. D. *Chem. Commun.* **2010**, *46*, 1013.
(21) Ozin, G. A.; Mccaffrey, J. G. *J. Phys. Chem.* **1984**, *88*, 645.
(22) Dugan, T. R.; Holland, P. L. *J. Organomet. Chem.* **2009**, *694*, 2825.
(23) Yu, Y.; Smith, J. M.; Flaschenriem, C. J.; Holland, P. L. *Inorg. Chem.* **2006**, *45*, 5742.
(24) Smith, J. M.; Sadique, A. R.; Cundari, T. R.; Rodgers, K. R.; Lukat-Rodgers, G.; Lachicotte, R. J.; Flaschenriem, C. J.; Vela, J.; Holland, P. L. *J. Am. Chem. Soc.* **2006**, *128*, 756.
(25) Yu, Y.; Sadique, A. R.; Smith, J. M.; Dugan, T. R.; Cowley, R. E.; Brennessel, W. W.; Flaschenriem, C. J.; Bill, E.; Cundari, T. R.; Holland, P. L. *J. Am. Chem. Soc.* **2008**, *130*, 6624.
(26) We particularly note the extensive reference collection in ref 22.
(27) Manuscript in preparation.
(28) Christiansen, J.; Goodwin, P. J.; Lanzilotta, W. N.; Seefeldt, L. C.; Dean, D. R. *Biochemistry* **1998**, *37*, 12611.
(29) Parkin, G. *J. Labelled Compd. Radiopharm.* **2007**, *50*, 1088.
(30) Parkin, G. *Acc. Chem. Res.* **2009**, *42*, 315.
(31) Glasoe, P. K.; Long, F. A. *J. Phys. Chem.* **1960**, *64*, 188.
(32) Davoust, C. E.; Doan, P. E.; Hoffman, B. M. *J. Magn. Reson., Ser. A* **1996**, *119*, 38.
(33) Brueggemann, W.; Niklas, J. R. *J. Magn. Reson., Ser. A* **1994**, *108*, 25.
(34) Lukoyanov, D.; Yang, Z. Y.; Duval, S.; Danyal, K.; Dean, D. R.; Seefeldt, L. C.; Hoffman, B. M. *Inorg. Chem.* **2014**, *53*, 3688.
(35) Lee, Y.; Kinney, R. A.; Hoffman, B. M.; Peters, J. C. *J. Am. Chem. Soc.* **2011**, *133*, 16366.
(36) Gunderson, W. A.; Suess, D. L.; Fong, H.; Wang, X.; Hoffmann, C. M.; Cutsail, G. E., III; Peters, J. C.; Hoffman, B. M. *J. Am. Chem. Soc.* **2014**, *136*, 14998.
(37) Lubitz, W.; Ogata, H.; Rudiger, O.; Reijerse, E. *Chem. Rev.* **2014**, *114*, 4081.
(38) Tai, H. L.; Nishikawa, K.; Suzuki, M.; Higuchi, Y.; Hirota, S. *Angew. Chem., Int. Ed.* **2014**, *53*, 13817.
(39) Bullock, R. M.; Bender, B. R. In *Encyclopedia of Catalysis*; Horváth, I. T., Ed.; Wiley: Hoboken, NJ, 2003; Vol. *4*, p 281.
(40) Mas-Ballesté, R.; Lledos, A. In *Comprehensive Inorganic Chemistry II*; Alvarez, S., Ed.; Elsevier Ltd.: Amsterdam, The Netherlands2013; Vol. *9*, p 736.
(41) Abu-Hasanayn, F.; Goldman, A. S.; Krogh-Jespersen, K. *J. Phys. Chem.* **1993**, *97*, 5890.
(42) Campian, M. V.; Perutz, R. N.; Procacci, B.; Thatcher, R. J.; Torres, O.; Whitwood, A. C. *J. Am. Chem. Soc.* **2012**, *134*, 3480.
(43) Wang, W. H.; Narducci, A. A.; House, P. G.; Weitz, E. *J. Am. Chem. Soc.* **1996**, *118*, 8654.
(44) Berberan-Santos, M. N.; Bodunov, E. N.; Valeur, B. *Chem. Phys.* **2005**, *315*, 171.
(45) Daniel, C. *J. Phys. Chem.* **1991**, *95*, 2394.
(46) Wang, W. H.; Weitz, E. *J. Phys. Chem. A* **1997**, *101*, 2358.
(47) We thank an anonymous reviewer for helping us to articulate this point.
(48) Hu, Y.; Lee, C. C.; Ribbe, M. W. *Science* **2011**, *333*, 753.
(49) Yang, Z. Y.; Moure, V. R.; Dean, D. R.; Seefeldt, L. C. *Proc. Natl. Acad. Sci. U. S. A.* **2012**, *109*, 19644.
(50) Seefeldt, L. C.; Yang, Z. Y.; Duval, S.; Dean, D. R. *Biochim. Biophys. Acta, Bioenerg.* **2013**, *1827*, 1102.
(51) Calladine, J. A.; Torres, O.; Anstey, M.; Ball, G. E.; Bergman, R. G.; Curley, J.; Duckett, S. B.; George, M. W.; Gilson, A. I.; Lawes, D. J.; Perutz, R. N.; Sun, X. Z.; Vollhardt, K. P. C. *Chem. Sci.* **2010**, *1*, 622.

DOI: 10.1021/jacs.5b11650
J. Am. Chem. Soc. 2016, 138, 1320−1327